

## He(I) PHOTOELECTRON SPECTROSCOPY OF THE GALLIUM MONOHALIDES

O. GRABANDT

*Akzo Research Laboratories, Velperweg 76, 6800 SB Arnhem, The Netherlands*

R. MOOYMAN

*Department of Physical Chemistry, Free University, De Boelelaan 1083, 1081 HV Amsterdam, The Netherlands*

and

C.A. DE LANGE

*Laboratory for Physical Chemistry, University of Amsterdam, Nieuwe Achtergracht 127, 1018 WS Amsterdam, The Netherlands*

Received 30 October 1989; in final form 18 January 1990

He(I) photoelectron spectra of the entire series of short-lived gallium monohalides produced in new solid-state reactions are presented. In addition, a high-resolution He(I) photoelectron spectrum of monomeric gallium trichloride is obtained. Hartree-Fock-Slater calculations are used as an aid in the interpretation of the experimental results.

### 1. Introduction

Photoelectron spectroscopy (PES) has been used extensively as a suitable method for obtaining information about the electronic structure of neutral and ionic states of small molecules in the gas phase. The study of short-lived or transient species by PES is a challenging task which is complicated by the inherent insensitivity and aselectivity of the technique. Despite such problems a large variety of PE studies has been carried out in which short-lived species have been produced using microwave discharges, high temperature evaporation, rapid gas phase reactions and laser dissociation methods. In addition it has been shown that "solid-state" reactions can provide a successful approach to the study of short-lived and reactive molecules as indicated by work on group III and group IV halides [1,2].

Focusing our attention on group III halides it should be realized that despite their short-lived and rather elusive character the gallium and indium monohalides have nonetheless appreciable technological importance. They play a vital role in the development of new semiconductor devices in high-

frequency and opto-electronic applications. In chemical vapour deposition techniques such as the Effer process [3] gallium and indium monohalides act as gas phase transporters of semiconductor material. The spectroscopy of the monohalides can therefore be of relevance for the development of laser diagnostic tools to optimize and control chemical vapour deposition techniques [4,5].

Several PE studies of group III monohalides have been reported. Of the transient boron and aluminium monohalides, BF [6] and AlF [7] were produced using high-temperature gas phase reactions. The PE spectrum of the transient species InF has been obtained recently [2]. The other indium monohalides as well as the corresponding thallium compounds are stable and could be studied by evaporation from the solid [8–10]. Throughout these studies the PE spectra of the group III monohalides were consistent with a predominantly ionic chemical bond scheme.

Gallium monohalides have been the subject of a large range of spectroscopic studies. Several optical absorption and emission studies were concerned with the ground and low-lying excited states of the neutral

species [11–18], leading to information about the energetics, vibrational frequencies, rotational constants, equilibrium bond lengths and dissociation energies. Detailed microwave spectroscopy studies have been carried out for all the ground state gallium monohalides [19–26]. Recently the development of emission and absorption spectroscopy of the monohalides as an analytical tool to quantitatively determine halide concentrations has drawn great interest [27–34]. Due to the transient nature of the gallium monohalides studies on ionic states have been limited. One investigation concerned with optical emission between low-lying ionic states has been reported recently [35].

In the present paper the He(I) photoelectron spectra of the entire series of gallium monohalides are presented. Appropriate “solid-state” reactions have proved to be particularly successful to produce GaF in the gas phase in the virtual absence of other gas phase products. The PE spectra of GaCl, GaBr and GaI were mixed with signals arising from the corresponding trihalides which were produced in the reactions as well. In addition, a high-resolution PE spectrum of the gallium trichloride in its unstable monomeric form was obtained.

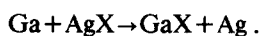
## 2. Experimental

The spectra of the gallium monohalides were measured on a home-built photoelectron spectrometer [36]. In the design of this spectrometer much attention has been given to features which are crucial in the study of short-lived and reactive species such as modularity, fast pumping and possibilities for easy disassembly, cleaning of critical parts of the system and reassembly. The spectrometer consists of two vacuum chambers, viz. the ionization chamber and the analyzer chamber, which are connected by a narrow slit ( $0.5 \times 10$  mm). A helium dc discharge lamp which produces mainly ( $\approx 98\%$ ) He(I $\alpha$ ) radiation of 21.218 eV is mounted on the ionization chamber. The photoelectrons pass from the ionization chamber through the slit into the analyzer chamber where a hemispherical kinetic energy analyzer is mounted. The photoelectrons are detected by a Mullard B419L channeltron electron multiplier. To ensure proper vacuum conditions, both chambers are pumped sep-

arately. To counteract the adverse effects associated with the reactivity of the short-lived species towards the spectrometer system, two measures were taken. First, all critical surfaces of the spectrometer, including the ionization chamber itself, were coated with colloidal graphite (DAG 580, Acheson Colloids Co.). Secondly, the drift in the PE spectra caused by the remaining local charge-up owing to the deposition of material on critical parts was suppressed by the use of a computer lock procedure [37].

Several production methods of group III monohalides have been reported in previous studies. Gallium monofluoride has been obtained as a reaction product from mixing gallium metal with AlF<sub>3</sub> [38] or CaF<sub>2</sub> [18] and heating to  $\approx 1000^\circ\text{C}$ . Also, passing HF over heated ( $\approx 800^\circ\text{C}$ ) gallium resulted in the formation of GaF [39]. The GaX (X = Br, Cl and I) species have been produced by mixing the metal with halogen containing compounds and subsequent heating, i.e. InX<sub>3</sub> ( $\approx 350^\circ\text{C}$ ) [19], PbX<sub>2</sub> ( $\approx 300^\circ\text{C}$ ) [23,25], GaCl<sub>3</sub> ( $\approx 1100^\circ\text{C}$ ) [12], by reacting heated gallium with a gas flow, i.e. of CCl<sub>4</sub> ( $\approx 1500^\circ\text{C}$ ) [26] or Br<sub>2</sub> ( $\approx 1000^\circ\text{C}$ ) [24] or by using gas discharge methods with Br<sub>2</sub> [15], I<sub>2</sub> [16] or GaBr<sub>3</sub> [17]. Most of these methods suffer from one or more disadvantages when used in combination with PES. To maximize the yield of the desired reaction product a stoichiometric gas phase mixture is required which is difficult to realize when starting from the solid. Also, in PES all components present in a gas phase mixture are detected which can often lead to undesired spectral overlap problems. Moreover, from the experimental point of view low temperature production methods are preferred.

In the recent past, “solid-state” reactions have been applied successfully in PES [1,2]. In the present study two reactions were exploited. First, the reaction of Ga with lead dihalides was tested. Secondly, in view of the successful production of InF [2] the same reaction was repeated in the gallium case:



The latter approach proved especially well suited for generating GaF in the virtual absence of other gas phase components.

A special oven system, designed to implement solid-state reactions, was mounted inside the ionization chamber, thereby ensuring short transport distances

of reaction products to the ionization region. Details of this oven system have been published before [2].

The following chemicals were obtained commercially: gallium metal ingots (Ventron, > 99.99%), silver(I) fluoride powder (Ventron, > 99%), silver(I) iodide (BDH Chemicals Ltd.), lead(II) bromide (Johnson Matthey Chem. Ltd., > 98%), lead(II) chloride and lead(II) iodide (BDH Chemicals Ltd., 99%), potassium chloride and potassium bromide (J.T. Baker, analyzed grade) and silver(I) nitrate (Johnson Matthey Chem. Ltd.). Silver(I) chloride and silver(I) bromide were prepared by precipitation from solution and washing. The noble gases argon (Matheson, > 99.999%) and krypton (Matheson, > 99.95%) were added to provide computer lock signals and for calibration.

The oven was filled with a mixture of gallium metal and silver(I) halide (molar ratio 1:1) or lead(II) halide (molar ratio 2:1). The oven power settings at which the gallium monohalide spectra appeared were between 15 and 45 Watt, corresponding to temperatures in the range of 700 to 900°C. The inner ionization chamber [2], in which the oven exits and which is mounted on the helium lamp, was heated separately. In the gallium chloride case, when this inner ionization chamber was kept at low temperature, the PE spectrum of the gallium trichloride monomer appeared. At higher temperatures increased gallium monochloride signals were observed. All spectra were obtained in the multiscan mode with total measuring times ranging between 20 and 60 min. Calibration of the spectra was performed using Kr (both He(I $\alpha$ ) and He(I $\beta$ )) and N<sub>2</sub> (GaF), Ar, HCl and N<sub>2</sub> (GaCl and GaCl<sub>3</sub>), Ar and GaBr<sub>3</sub> (GaBr) and Ar and GaI<sub>3</sub> (GaI). The resolution of the spectra could be maintained between 30 and 50 meV.

### 3. Computational

To aid in the assignment, Hartree-Fock-Slater (HFS) LCAO calculations were performed on the gallium monohalides. Several features incorporated in these calculations have proven to give reliable ionization energies (IEs) and chemical bond structure information of relatively complicated molecules. The non-local HF exchange potential has been replaced by a local X $\alpha$  exchange potential [40]. The molecu-

lar orbitals are expanded in atomic orbitals. The HFS equations are solved by the method of Baerends et al. [41] combined with an efficient numerical integration algorithm [42]. A Slater type basis set was used with single zeta core functions for orthogonalization and triple zeta quality valence functions. The cores were kept frozen up to Ga 3p, F 1s, Cl 2p, Br 3p and I 4p. The number of integration points used was 744 in the GaI case and 684 for the other monohalides. The Slater transition state method [43] was used to calculate ionization energies. In this method half an electron is removed from the orbital out of which ionization takes place.

In compounds consisting of heavy elements spin-orbit coupling is anticipated to become significant. Relativistic effects were incorporated in the HFS calculations using a perturbational treatment of these effects on the valence orbitals developed by Snijders et al. [44,45]. The core orbitals were calculated by fully numerical Dirac-Fock-Slater calculations.

With these methods potential energy curves were calculated for the neutral ground state (X <sup>1</sup> $\Sigma^+$ ) and three low-lying ionic states (X <sup>2</sup> $\Sigma^+$ , A <sup>2</sup> $\Pi_{1/2,3/2}$ , B <sup>2</sup> $\Sigma^+$ ) of the monohalides. The potential energy curves were calculated using a 0.1 au internuclear distance grid. The internuclear distances considered ranged between 2.4 and 5.2 (GaF), 2.6 and 5.6 (GaCl), 3.0 and 6.5 (GaBr) and 3.0 and 6.3 au (GaI). To obtain smooth curves a cubic spline fit interpolation procedure was used [46]. Compared to polynomial fits, cubic spline fits have the advantage of smooth behaviour over the entire point interval. In the bound states the vibrational problem was solved using a Numerov integration scheme [47] incorporated in vibrational eigenvalue calculations [48,49]. By assuming an electronic transition moment independent of internuclear distance Franck-Condon (FC) factors were obtained by calculating the overlap integral between vibrational wavefunctions in the neutral ground state and those in the ionic states. As an alternative to these FC calculations in the GaF case band simulations starting from Morse potentials were found to be useful. Experimental data concerning the neutral ground state together with the measured vibrational frequency of the X <sup>2</sup> $\Sigma^+$  ionic state were used. The equilibrium bond length was varied stepwise (0.02 au). In each step the vibrational wavefunctions and FC factors were calculated

leading to a simulated PE band shape. By comparison with experiment a reliable estimate of the equilibrium bond length in this ionic state could be obtained. The vibrational calculations were performed assuming mass 68.9 (Ga), 19.0 (F), 35.0 (Cl), 78.9 (Br) and 126.9 (I) (all in amu) (60%, 100%, 76%, 51% and 100% natural abundance respectively).

#### 4. Results and discussion

A simple MO picture of the gallium monohalides can be formed on the basis of the valence orbital energies of the constituent atoms. The electron configurations are Ga  $4s^2 4p$  and X  $np^5$  for the respective halogen atoms (X=F, Cl, Br, I;  $n=2-5$ ). In the He(I) region three doubly occupied MOs are expected: a  $\sigma$  orbital (HOMO) with mainly Ga character but with increasing halogen participation in going from F to I, a doubly degenerate  $\pi$  orbital of predominantly halogen lone pair character and a bonding  $\sigma$  MO.

In fig. 1 the experimental PE spectrum obtained in the reaction between Ga and AgF is shown. Three ionization bands which varied simultaneously with oven temperature are attributed to GaF. A small signal due to some  $N_2$  leakage into the spectrometer is indicated. In addition, strong signals due to  $SiF_4$  are visible. However, the PE bands of  $SiF_4$  which corre-

spond to ionizations from fluorine lone pair orbitals appear only at high ionization energies ( $> 16$  eV) and do not interfere with the GaF ionization phenomena. No signals were observed from  $GaF_3$ .

The first band assigned to GaF appears between 10.5 and 11.0 eV. This band is enlarged in fig. 2 and shows five components. The distance between the first and second component is  $605 \pm 25$   $cm^{-1}$  which corresponds to the vibrational frequency associated with the neutral ground state [18]. Apparently, hot GaF is produced in the solid-state reaction and photoionization not only from  $v''=0$  but also from  $v''=1$  is observed. The feature at 10.56 eV is therefore ascribed to a hot band transition. The low spectral intensity and the hot band contributions result in a somewhat irregular vibrational progression associated with the lowest ionic state with a spacing of  $745 \pm 25$   $cm^{-1}$ . Clearly, upon photoionization the vibrational frequency in the ionic state shows an increase compared to that of the ground state. The adiabatic ionization energy corresponds to the position of the second component at 10.64 eV. The third component shows the largest intensity and is measured at 10.74 eV.

The second band between 12.9 and 14.5 is broad and no structure is resolved. The band onset is estimated at 12.91 eV, the band maximum is measured at 13.61 eV. The krypton signals which partly overlap this band were required for lock purposes. The third

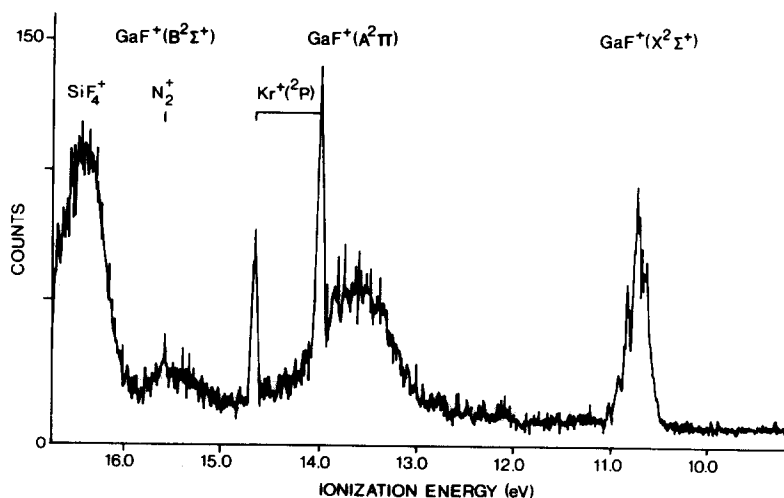


Fig. 1. He(I) photoelectron spectrum of GaF with krypton added as a reference.

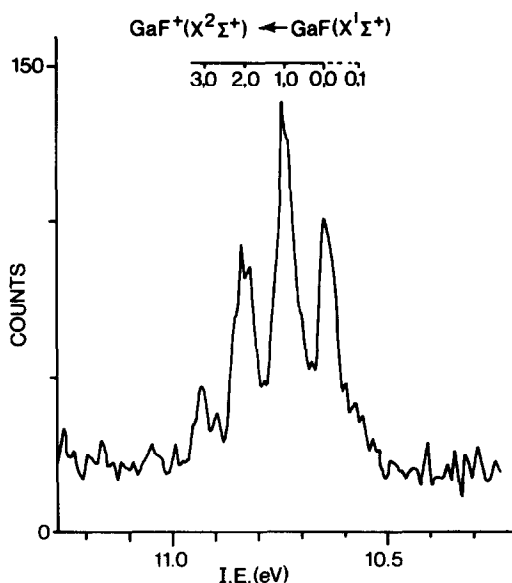


Fig. 2. Expanded photoelectron spectrum of the ionization process  $\text{GaF}^+(\text{X}^2\Sigma^+) \leftarrow \text{GaF}(\text{X}^1\Sigma^+)$ .

band between 15.0 and 15.8 eV is a low intensity, structureless band with the band onset at approximately 15.07 eV and its maximum at 15.41 eV.

Next, the PE spectra resulting from the reaction between Ga and AgCl are presented. Several compounds formed in this reaction could be identified in the gas phase in a series of experiments on the basis

of their PE spectra. At low oven temperatures the  $\text{GaCl}_3$  dimer dominated [50,51]. Raising the oven temperature led to a pure spectrum of monomeric  $\text{GaCl}_3$  which is presented in fig. 3. At comparatively high temperatures of oven and inner ionization chamber mixtures of monomeric  $\text{GaCl}_3$  and a new unstable compound assigned as GaCl were observed. A representative PE spectrum of the latter situation is presented in fig. 4.

Careful inspection of intensity variations as a function of temperature indicated that three spectral features (see fig. 4) behaved in a similar fashion. The first feature with the band onset at 9.91 eV and the band maximum at 10.07 eV is clearly identified and ascribed to the first band of GaCl. Although in all experiments some band structure consistently appeared, the resolution was not sufficient to obtain a reliable value for a vibrational spacing. A large and broad PE feature also assigned to GaCl has a band onset at 10.80 eV and band maximum at 11.38 eV. It shows partial overlap with  $\text{GaCl}_3$  signals. The third band of GaCl could be located at 14.05 eV despite the fact that it is heavily masked by  $\text{GaCl}_3$  signals. Small signals at 12.8 eV are assigned to HCl which is probably formed in the reaction of AgCl with traces of moisture in the oven. Argon was used as the lock signal.

In fig. 5 the PE spectrum of the products formed in the reaction between Ga and  $\text{PbBr}_2$  is shown. The spectrum arises from a gas phase mixture of  $\text{GaBr}_3$

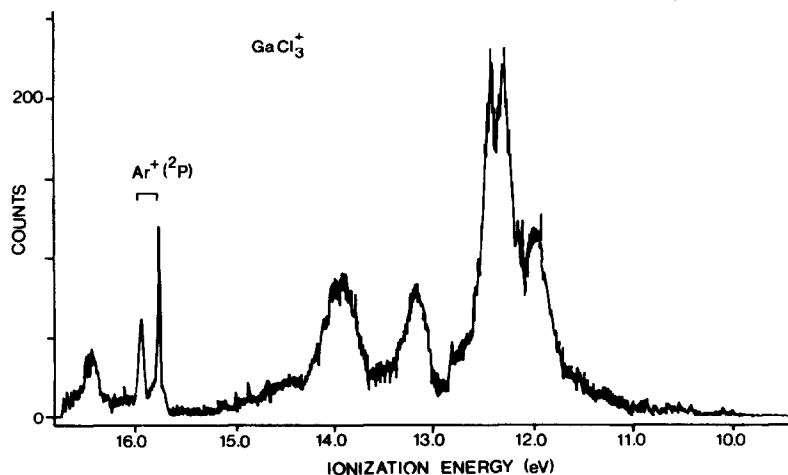


Fig. 3. He(I) photoelectron spectrum of monomeric  $\text{GaCl}_3$  with argon added as a reference.

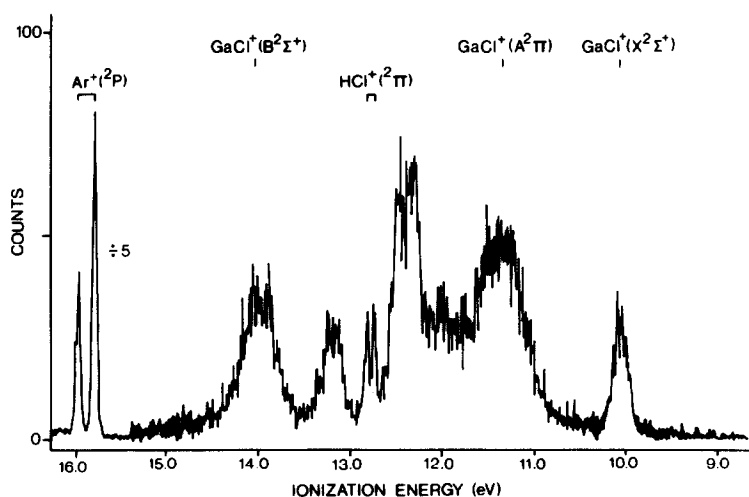


Fig. 4. He(I) photoelectron spectrum of a mixture of GaCl and GaCl<sub>3</sub>.

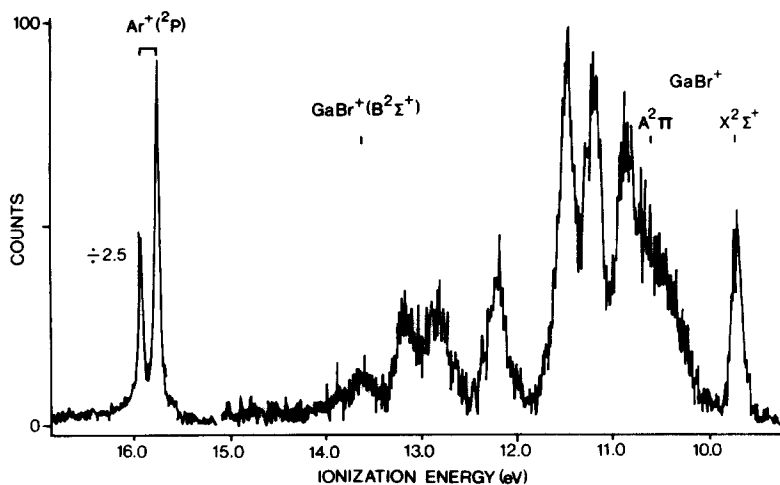


Fig. 5. He(I) photoelectron spectrum of a mixture of GaBr and GaBr<sub>3</sub>.

[50] and a new unstable compound assigned as GaBr. Three GaBr bands can be clearly identified from their similar behaviour as a function of temperature. Argon was used as the lock signal. In the first GaBr band with onset at 9.58 eV and maximum at 9.72 eV no vibrational structure is resolved. A broad second band with its onset at 10.14 eV and centered at 10.60 eV is partly obscured by the GaBr<sub>3</sub> band system arising from photoionization of Br lone pair MOs. A careful comparison of several spectra obtained under different conditions in which the GaBr<sub>3</sub> contributions could

be varied slightly provides experimental evidence for the presence of a splitting. This splitting, originating from spin-orbit coupling, leads to two band maxima estimated at 10.45 and 10.75 eV. A third structureless GaBr band with low intensity is observed with a band onset at 13.45 and its maximum at 13.62 eV.

Fig. 6 shows the experimental result of the reaction of Ga with PbI<sub>2</sub> at high temperature. Around 14 eV argon signals from He(Iβ) radiation are observed. The relatively sharp signal at 12.6 eV is probably due to evaporation of traces of water included in PbI<sub>2</sub>.

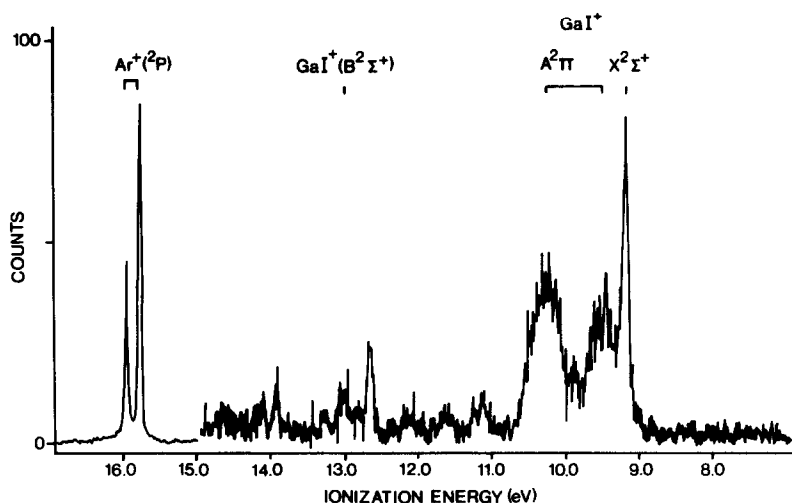


Fig. 6. He(I) photoelectron spectrum of GaI.

Most of the low intensity signals present in this spectrum can be attributed to  $\text{GaI}_3$  [50]. Three spectral features are assigned to GaI. The first band (onset at 9.03 eV, maximum at 9.19 eV) is sharp and does not show vibrational structure as expected because of the large reduced mass. The transition to the second ionic state is now clearly split into two spin-orbit components with maxima at 9.49 and 10.25 eV. A third band of low intensity, with band onset at 12.81 eV and band maximum at 12.98 eV is finally assigned to GaI on the basis of its behaviour as a function of temperature.

The experimental PE results for the gallium monohalides are summarized in table 1.

In fig. 7 the HFS calculated potential energy curves

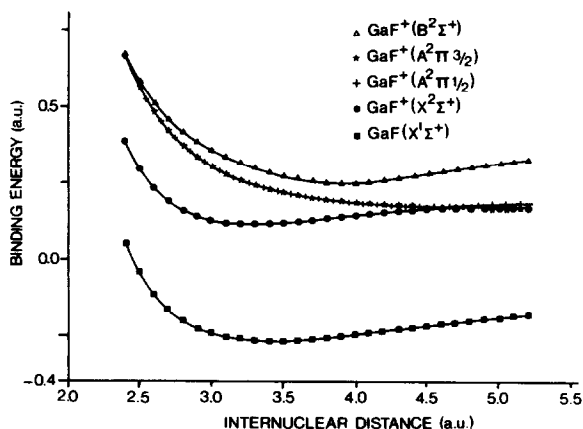


Fig. 7. Hartree-Fock-Slater potential energy curves for the neutral ground state and the lowest ionic states of GaF.

of neutral and ionic states of GaF are presented. Since the computational results for the entire series of gallium monohalides show the same overall structure, GaF is chosen as an illustrative example. The neutral ground state ( $X^1\Sigma^+$ ) is bound. The lowest ionic state ( $X^2\Sigma^+$ ) is also bound with an equilibrium bond length slightly shorter than that of the neutral ground state. The first excited ionic state ( $A^2\Pi$ ) is dissociative throughout the series. The spin-orbit splitting in this state shows a significant increase with halogen mass. The  $B^2\Sigma^+$  ionic state is bound with its equilibrium bond length shifted towards larger internuclear distances.

The quality of these computed potential energy curves can be judged by comparing calculated equilibrium bond lengths, associated vibrational frequencies and their anharmonicities with experimental data. Such experimental data are only available for the neutral ground states of the gallium monohalides. A comparison of calculated and experimental results for the four ground states is given in table 2. As a general trend the calculated bond lengths are somewhat larger and the vibrational frequencies slightly lower than those obtained from experiment. The agreement between theoretical and experimental anharmonicities is excellent. The present underestimation of the HFS calculated bond lengths was also found in the InF case [2]. The calculated equilibrium bond lengths for the ionic states under consideration are

Table 1  
Experimental and HFS calculated ionization energies, in eV, of the four gallium monohalides

	GaF		GaCl		GaBr		GaI	
	exp.	calc.	exp.	calc.	exp.	calc.	exp.	calc.
$X^2\Sigma^+$	10.64 <sup>a,b)</sup>	10.45 <sup>a)</sup>	9.91	9.64	9.58	9.23	9.03	8.60
	10.74 <sup>b,c)</sup>	10.45 <sup>c)</sup>	10.07	9.68	9.72	9.23	9.19	8.60
$A^2\Pi_{3/2}$	12.91 <sup>d,e)</sup>	–	10.80	–	10.14 (10.14) <sup>f)</sup>	–	–	–
	13.61 <sup>c,e)</sup>	13.65 <sup>c)</sup>	11.38	10.74	10.60 (10.45) <sup>f)</sup>	9.88	9.49	8.94
$A^2\Pi_{1/2}$	12.91 <sup>d,e)</sup>	–	10.80	–	10.14 (–) <sup>f)</sup>	–	9.93	–
	13.61 <sup>c,e)</sup>	13.69 <sup>c)</sup>	11.38	10.82	10.60 (10.75) <sup>f)</sup>	10.24	10.25	9.64
$B^2\Sigma^+$	15.07 <sup>d,e)</sup>	14.17 <sup>a)</sup>	–	13.53	13.45	13.40	12.81	13.03
	15.41 <sup>c,e)</sup>	15.16 <sup>d)</sup>	14.05	13.59	13.62	13.44	12.98	13.03

<sup>a)</sup> Adiabatic transition. <sup>b)</sup>  $\pm 0.01$  eV. <sup>c)</sup> Band maximum.

<sup>d)</sup> Band onset. <sup>e)</sup>  $\pm 0.04$  eV. <sup>f)</sup> Indications for spin-orbit splitting.

also presented in table 2 for all members of the series. Moreover, the vibrational frequency and anharmonicity calculated for  $X^2\Sigma^+$  in  $\text{GaF}^+$  are given as well.

From the HFS calculated potential energy curves adiabatic and vertical IEs have been obtained throughout the series. From previous experience [52] calculated vertical IEs and experimental values generally correspond to within  $\approx 1$  eV, while differences between bands often agree to within  $\approx 0.3$  eV. A comparison of experimental and calculated IEs in table 1 lends strong support to an assignment which attributes the present PE spectra to the gallium mono-

halides. In the case of GaCl IEs have been calculated using a more sophisticated Green's function method [53]. The results presented in the Green's function calculations support the above picture ( $X^2\Sigma^+$ : 9.68 eV,  $A^2\Pi$ : 11.25 eV,  $B^2\Sigma^+$ : 14.10 eV).

Resolved vibrational structure has only been observed in the ionization to the ground ionic state  $X^2\Sigma^+$  in  $\text{GaF}^+$ . The HFS calculations predict a shortening of the equilibrium bond length upon ionization to  $r_e = 3.27$  au starting from a value of  $r_e = 3.40$  au in the neutral ground state. Solving the vibrational problem in the HFS  $X^2\Sigma^+$  potential energy curve

Table 2  
Comparison of experimental and HFS calculated vibrational frequencies, anharmonicities and equilibrium bond lengths

	$\omega_e$ (exp.) ( $\text{cm}^{-1}$ )	$\omega_e$ (calc.) ( $\text{cm}^{-1}$ )	$\omega_e x_e$ (exp.) ( $\text{cm}^{-1}$ )	$\omega_e x_e$ (calc.) ( $\text{cm}^{-1}$ )	$r_e$ (exp.) (au)	$r_e$ (calc.) (au)
$\text{GaF}(X^1\Sigma^+)$	622 [18]	592	3.2 [18]	3.1	3.353 [20]	3.40
$\text{GaF}^+(X^2\Sigma^+)$	$745 \pm 25$	655	–	4.5	$3.18 \pm 0.005$	3.27
$\text{GaF}^+(B^2\Sigma^+)$	–	–	–	–	–	3.91
$\text{GaCl}(X^1\Sigma^+)$	366 [26]	342	1.3 [26]	1.2	4.161 [26]	4.25
$\text{GaCl}^+(X^2\Sigma^+)$	–	390	–	–	–	4.07
$\text{GaCl}^+(B^2\Sigma^+)$	–	–	–	–	–	4.44
$\text{GaBr}(X^1\Sigma^+)$	267 [24]	251	0.7 [24]	0.7	4.446 [24]	4.50
$\text{GaBr}^+(X^2\Sigma^+)$	–	–	–	–	–	4.41
$\text{GaBr}^+(B^2\Sigma^+)$	–	–	–	–	–	4.68
$\text{GaI}(X^1\Sigma^+)$	216 [23]	208	0.5 [23]	0.5	4.866 [19]	4.81
$\text{GaI}^+(X^2\Sigma^+)$	–	–	–	–	–	4.84 <sup>a)</sup>
$\text{GaI}^+(B^2\Sigma^+)$	–	–	–	–	–	4.90

<sup>a)</sup> Reliability questionable due to convergence problems.

leads to a vibrational frequency of  $655\text{ cm}^{-1}$  and an anharmonicity of  $4.5\text{ cm}^{-1}$ . This frequency is significantly lower than that of  $745\text{ cm}^{-1}$  observed in the PE spectrum. Moreover, calculating FC factors from the HFS potential energy curves predicts a rather short vibrational progression with  $v^+ = 0 \leftarrow v'' = 0$  as the most intense component, in contrast to the observed transition. The calculated PE intensities of the components of the progression are highly sensitive to the difference in equilibrium internuclear distances between the potential energy curves involved. By using the Morse potential approach described in the computational section a good  $r_e$  value of the  $X^2\Sigma^+$  state in  $\text{GaF}^+$  can be extracted. The  $X^1\Sigma^+$  ground state potential energy curve was treated as a Morse potential with  $r_e = 3.35\text{ au}$  [20],  $\omega_e = 622\text{ cm}^{-1}$  [18] and  $\omega_e x_e = 3.2\text{ cm}^{-1}$  [18]. To define a Morse potential for  $X^2\Sigma^+$  our experimental value of  $\omega_e = 745\text{ cm}^{-1}$  together with an anharmonicity of  $5.8\text{ cm}^{-1}$  was chosen. With this anharmonicity a Morse potential is constructed with the same dissociation energy as calculated from the HFS curve. PE band simulations including hot band contributions from  $v'' = 1$  were performed. Excellent and unambiguous agreement with the experimental band shape could be obtained using  $r_e(X^2\Sigma^+) = 3.18 \pm 0.005\text{ au}$  and a temperature of  $650 \pm 100^\circ\text{C}$  in the photoionization region.

When the first experimental IEs of the gallium monohalides are plotted as a function of the first atomic halogen IEs [54] a roughly linear decrease is observed. This indicates significant halogen character of the highest occupied MO. As in the  $\text{InF}$  case [2] an unusual bond strength increase is observed upon ionization and a similar explanation can be advanced. The calculations show a large charge separation in the neutral ground state of  $\text{GaF}$ , i.e.  $\text{Ga} + 0.5 e$ ,  $\text{F} - 0.5 e$ . This charge separation becomes less important towards  $\text{GaI}$ , viz.  $\text{Ga} + 0.2 e$ ,  $\text{I} - 0.2 e$ . In  $\text{GaF}$  all the charge removed upon ionization of the MO involved, is removed from that part of the MO centered on gallium, thereby increasing the ionic bond strength. A similar but less dramatic situation prevails in  $\text{GaCl}$  and  $\text{GaBr}$ . In contrast, in  $\text{GaI}$  the charge depletion on ionization is almost equally divided over both centers and no significant increase in ionic bond strength is predicted. The highest occupied MO is largely localized on Ga in  $\text{GaF}$  (60% Ga 4s; 10% Ga

4p<sub>z</sub>; 30% F 2p<sub>z</sub>). This localization becomes less important towards  $\text{GaI}$  (30% Ga 4s; 20% Ga 4p<sub>z</sub>; 50% I 5p<sub>z</sub>). The trends observed in charge depletion upon ionization, charge localization and orbital character rationalize the measured increase in vibrational frequency as observed in the first PE band of  $\text{GaF}$ . Although in the present study the vibrational frequencies associated with the lowest ionic states of the remaining gallium monohalides could not be measured, similar but less pronounced effects are expected in  $\text{GaCl}$  and  $\text{GaBr}$ . For  $\text{GaI}$  only small effects are predicted.

An estimate of the dissociation energies of the ionic ground state of the monohalides can be obtained on the basis of the dissociation energies of the neutral ground state, the lowest IE of atomic gallium and the IEs measured in this work. The dissociation products of the neutral ground states are assumed to be  $\text{Ga}(^2P_{1/2})$  and  $\text{X}(^2P)$ , of the ionic ground states  $\text{Ga}^+(^1S_0)$  and  $\text{X}(^2P)$ . Using the lowest IE of atomic gallium,  $\text{Ga}^+(^1S_0) \leftarrow \text{Ga}(^2P_{1/2})$ , of 6.00 eV [55] and literature values for the experimental dissociation energies of the neutral ground states, i.e. 5.98 ( $\text{GaF}$ ), 4.92 ( $\text{GaCl}$ ), 4.31 ( $\text{GaBr}$ ) and 3.47 eV ( $\text{GaI}$ ) [56], combination with the present IEs for  $\text{GaX}^+(X^2\Sigma^+) \leftarrow \text{GaX}(X^1\Sigma^+)$  (see table 1) leads to dissociation energies for the  $X^2\Sigma^+$  ionic state of  $D_0 = 10800$  ( $\text{GaF}^+$ ), 8200 ( $\text{GaCl}^+$ ), 5900 ( $\text{GaBr}^+$ ) and  $3600 \pm 500\text{ cm}^{-1}$  ( $\text{GaI}^+$ ) respectively.

The  $A^2\Pi$  ionic state is calculated to be dissociative. This is confirmed by the lack of observed vibrational structure in the PE spectra of all four monohalide species. The PE envelope of the transition to the first excited ionic state can be explained in terms of reflection of the  $v''$  vibrational wavefunction of the ground state neutral onto the dissociative potential of the  $A^2\Pi$  ionic state. This reflection leads to a Gaussian type PE envelope. Spin-orbit coupling in this state can lead to broadening or splitting of the observed band. In the atomic case the spin-orbit splitting in gallium equals  $826\text{ cm}^{-1}$  [57] which can in principle be resolved with PES. The atomic halogen splittings are 404, 881, 3685 and  $7603\text{ cm}^{-1}$  respectively [58], showing a dramatic increase towards the heavy elements. Unlike the situation in  $\text{GaF}$  and  $\text{GaCl}$ , in  $\text{GaBr}$  and  $\text{GaI}$  increasingly clear indications for a spin-orbit splitting are observed. This indicates a localization of the ionized MO on the hal-

ogen. The HFS calculations confirm this observation. The MO out of which ionization takes place ranges from 95% F  $2p_{x,y}$  in GaF to 90% I  $5p_{x,y}$  in GaI. Moreover, plotting the observed IEs for this orbital against the first atomic halogen IEs shows a strong and again roughly linear dependence, in line with the above conclusions. The observed spin-orbit splittings, 0.30 eV in GaBr and 0.76 eV in GaI, compare well with the HFS values, 0.36 and 0.70 eV respectively. The splittings calculated in GaF and GaCl, 0.04 and 0.08 eV, were not resolved in the present experiments. On the basis of the orbital composition of the ionized orbital the simple picture of combining the atomic spin-orbit splittings weighted by the square of the constituting atomic orbital coefficients leads to splittings in the  $A^2\Pi$  state of 0.05, 0.09, 0.39 and 0.76 eV going from gallium monofluoride to gallium monoiodide. This trend is well reproduced by the HFS results and is observed experimentally. The calculations indicate the  $A^2\Pi_{3/2}$  state to be energetically below  $A^2\Pi_{1/2}$ . The difference in intensity of the two spin-orbit components observed in GaI can be largely attributed to contributions from  $GaI_3$  signals. The HFS calculations show that the  $A^2\Pi$  ionic state dissociates into the same products as  $X^2\Sigma^+$ .

The HFS calculations predict the  $B^2\Sigma^+$  ionic states of the monohalides to be bound states. In all four PE spectra the transition from the neutral ground state to this ionic state is of low intensity. As a consequence of the poor signal-to-noise ratio no vibrational structure is resolved. In table 2 the calculated bond lengths are tabulated and found to increase upon ionization to this ionic state. The increase is very large in GaF and becomes smaller towards GaI. The large discrepancy between calculated and observed bandwidths shown in table 1 for GaF decreases throughout the series towards GaI. The large change in equilibrium bond length in GaF causes the transitions starting from  $v''=0$  towards the lower vibrational levels in the B ionic state to have negligible FC factors. Towards GaI the equilibrium bond lengths become similar, thereby eliminating this effect. In GaF the ionized orbital consists of 35% Ga 4s and 65% F, mainly F  $2p_z$ . On ionization a reduction of ionic bond strength and an increase of bond length are expected. In GaI, in contrast, the ionized orbital is already localized on Ga, i.e. 65% Ga 4s and 35% I, mainly I  $5p_z$ . Upon ionization charge depletion is calculated to be

divided equally over both centers, therefore no ionic bond strength change and a smaller change in equilibrium bond length are expected. Towards larger internuclear distances the ionized orbital becomes localized on Ga. The calculations indicate a dissociation towards  $Ga^+(^3P)$  and  $X(^2P)$ . An estimate of the dissociation energies of the B state can be obtained using the  $Ga^+(^3P) \leftarrow Ga(^2P_{1/2})$  IE of 11.9 eV [55] and the present IEs (see table 1) resulting in  $D_0=22700$  (GaF<sup>+</sup>), 23600 (GaCl<sup>+</sup>), 22300 (GaBr<sup>+</sup>) and  $20700 \pm 500$  cm<sup>-1</sup> (GaI<sup>+</sup>).

In a recent optical emission spectroscopy study transitions between ionic states in the gallium monohalides have been observed [35]. Throughout the series the transition  $X^2\Sigma^+ \leftarrow B^2\Sigma^+$  has been studied but no vibrational structure has been resolved. These transitions were located at 3.9 eV in GaF, 4.1 eV in GaCl and 3.8 eV in GaBr. These data can be compared with the present results by subtracting the band onsets for the first and third bands in the PE spectra. However, for  $B^2\Sigma^+$  in GaF<sup>+</sup> the band onset cannot be determined reliably as discussed before. The  $X^2\Sigma^+ \leftarrow B^2\Sigma^+$  transition energies obtained are 4.67, 3.98 and 3.90 eV respectively. As expected, the agreement for GaF<sup>+</sup> is rather poor. For GaCl<sup>+</sup> and GaBr<sup>+</sup> the results from both techniques agree well. In the optical emission study indications for an additional ionic state,  $C^2\Pi$ , which dissociates into  $Ga^+(^3P)$  and  $X(^2P)$  ( $X=Cl, Br$ ) were found in GaCl and GaBr. This would predict PE features at  $\approx 15.1$  eV (GaCl) and  $\approx 14.3$  eV (GaBr). The  $C^2\Pi$  ionic state was thought to differ in two electrons from the neutral ground state configuration [35]. In our work no evidence for  $C^2\Pi$  could be found and no HFS calculations for shake-up type ionic states were performed. The absence of a  $C^2\Pi$  feature in the PE spectra can be explained because it involves a two-electron transition from the neutral ground state and since in addition a rather large decrease in equilibrium bond length is expected on ionization, thereby reducing the intensity of the transition below the detection limit in the present experiment.

The gallium trihalides are known to dimerize in the gas phase at low temperatures. In a PE study of the  $GaX_3$  ( $X=C, Br$  and I) species [50], pure spectra of monomeric GaBr<sub>3</sub> and GaI<sub>3</sub> have been obtained. However, the PE spectrum assigned to monomeric GaCl<sub>3</sub> showed very broad ionization features indi-

Table 3  
Comparison of experimental ionization energies of GaCl<sub>3</sub> and the results of Green's function calculations [53]

	Calc. (eV)	Exp. (eV) band maximum
a <sub>2</sub> '	11.96	11.98
e'	12.24	12.31
e''	12.22	12.44
a <sub>2</sub> ''	13.22	13.17
e'	13.96	13.91
a <sub>1</sub> '	16.39	16.43

cating an appreciable dimer contribution. In a parallel PE study [51] on the dimerization of GaX<sub>3</sub> species in the gas phase, various dimer–monomer mixtures of GaCl<sub>3</sub> have been obtained as a function of temperature and a relatively pure monomer spectrum, albeit at low resolution, has been reported. In fig. 3 a high-resolution PE spectrum of mainly monomeric GaCl<sub>3</sub> obtained in our work is presented. Following the analysis by Dehmer et al. [50] the PE features in the range between 11 and 14 eV are due to MOs consisting of halogen p-type atomic orbitals. Semi-empirical [50] and Green's function [53] calculations have shown the e' and e'' ionic states to be nearly degenerate. On symmetry grounds the e' can split into two spin-orbit components. The experimental spectrum shows a separation of 0.13 eV between the e' and e'' states. However, no experimental evidence of spin-orbit coupling in the e' state (at 12.31 eV) is observed. In table 3 the excellent agreement between our experimental IEs and the Green's function results is illustrated.

## 5. Conclusion

He(I) photoelectron spectra of the transient GaX (X = F, Cl, Br and I) species, produced via solid-state reactions, have been recorded and interpreted on the basis of ab initio HFS calculations. Three ionic states of all four monohalides have been identified. In addition a high-resolution PE spectrum of monomeric, unstable GaCl<sub>3</sub> has been obtained.

## Acknowledgement

The authors are grateful to the Netherlands Organization for Scientific Research (NWO) for equipment grants and financial support (OG), to P. Vernooijs for computational assistance and to Professor Ch. Ottinger for helpful discussions.

## References

- [1] G. Jonkers, S.M. van der Kerk and C.A. de Lange, *Chem. Phys.* 70 (1982) 69.
- [2] O. Grabandt, C.A. de Lange and R. Mooyman, *Chem. Phys. Letters* 160 (1989) 359.
- [3] D. Effer, *J. Electrochem. Soc.* 112 (1965) 1020.
- [4] V.M. Donnelly and R.F. Karliceck, *J. Appl. Phys.* 53 (1982) 6399.
- [5] R.F. Karliceck, B. Hammarlund and J. Ginocchio, *J. Appl. Phys.* 60 (1986) 794.
- [6] J.M. Dyke, C. Kirby and A. Morris, *J. Chem. Soc. Faraday Trans. II* 79 (1983) 483.
- [7] J.M. Dyke, C. Kirby, A. Morris, B.W.J. Gravenor, R. Klein and P. Rosmus, *Chem. Phys.* 88 (1984) 289.
- [8] J. Berkowitz and J.L. Dehmer, *J. Chem. Phys.* 57 (1972) 3194.
- [9] J. Berkowitz and T.A. Walter, *J. Chem. Phys.* 49 (1968) 1184.
- [10] J. Berkowitz, *J. Chem. Phys.* 56 (1972) 2766.
- [11] D. Welti and R.F. Barrow, *Nature* 4265 (1951) 161.
- [12] F.K. Levin and J.G. Winans, *Phys. Rev.* 84 (1951) 431.
- [13] D. Welti and R.F. Barrow, *Proc. Phys. Soc. (London)* A 65 (1952) 629.
- [14] R.F. Barrow, J.A.T. Jacquest and E.W. Thompson, *Proc. Phys. Soc. (London)* A 67 (1954) 528.
- [15] T. Savithry, D.V.K. Rao, A.A.N. Murty and P.T. Rao, *Physica* 75 (1974) 386.
- [16] G. Lakshminarayana and A. Sethumadhavan, *J. Quant. Spectry. Radiative Transfer* 23 (1980) 343.
- [17] J. Borkowska-Burnecka and W. Zyrnicki, *Physica C* 100 (1980) 124.
- [18] W.B. Griffith Jr., G.A. Bickel, H.D. McSwiney and C. Weldon Mathews, *J. Mol. Spectry.* 104 (1984) 343.
- [19] A.H. Barret and M. Mandel, *Phys. Rev.* 109 (1958) 1572.
- [20] J. Hoeft, F.J. Lovas, E. Tiemann and T. Törring, *Z. Naturforsch.* 25a (1970) 1029.
- [21] J. Hoeft, F.J. Lovas, E. Tiemann and T. Törring, *Z. Angew. Physik* 31 (1971) 265.
- [22] S. Pfaffe, E. Tiemann and J. Hoeft, *Z. Naturforsch.* 33a (1978) 1386.
- [23] K.P.R. Nair, H.U. Schütze-Pahlmann and J. Hoeft, *Chem. Phys. Letters* 70 (1980) 583.
- [24] K.P.R. Nair, H.U. Schütze-Pahlmann and J. Hoeft, *Chem. Phys. Letters* 80 (1981) 149.
- [25] K.P.R. Nair and J. Hoeft, *J. Mol. Spectry.* 85 (1981) 301.

- [26] J. Hoefl and K.P.R. Nair, *Z. Physik D* 4 (1986) 189.
- [27] K. Dittrich, *Anal. Chim. Acta* 97 (1978) 59.
- [28] G. Henrion and D. Marquardt, *Z. Chemie* 18 (1978) 190.
- [29] K. Dittrich and S. Schneider, *Anal. Chim. Acta* 115 (1980) 189.
- [30] K. Tsunoda, H. Haraguchi and K. Fuwa, *Spectrochim. Acta B* 35 (1980) 715.
- [31] D. Marquardt, R. Stösser and G. Henrion, *Spectrochim. Acta B* 36 (1981) 951.
- [32] K. Dittrich, B. Vorberg, J. Funk and V. Beyer, *Spectrochim. Acta B* 39 (1984) 349.
- [33] K. Tsunoda, H. Haraguchi and K. Fuwa, *Spectrochim. Acta B* 40 (1985) 1651.
- [34] Z.M. Kassir, A.A.H. Ta'abi, A.T. Al-Samaraie and T.A.K. Nasser, *Anal. Chim. Acta* 172 (1985) 323.
- [35] Th. Glenewinkel-Meyer, A. Kowalski, B. Müller, Ch. Ottinger and W.H. Beckenridge, *J. Chem. Phys.* 89 (1988) 7112.
- [36] D.M. de Leeuw, Ph.D. Thesis, Vrije Universiteit, Amsterdam, The Netherlands (1979).
- [37] O. Grabandt, H.G. Muller and C.A. de Lange, *Comput. Enhanced Spectry*, 2 (1984) 33.
- [38] R. Honerjäger and R. Tischer, *Z. Naturforsch.* 29a (1974) 1919.
- [39] H.G. Schnöckel and H.J. Göcke, *J. Mol. Struct.* 50 (1978) 281.
- [40] J.C. Slater, *Phys. Rev.* 81 (1951) 385; 91 (1953) 528.
- [41] E.J. Baerends, D.E. Ellis and P. Ros, *Chem. Phys.* 2 (1973) 41.
- [42] P.M. Boerrigter, Ph.D. Thesis, Vrije Universiteit, Amsterdam, The Netherlands (1987).
- [43] J.C. Slater, *The Self Consistent Field for Molecules and Solids*, Vol. 4 (McGraw-Hill, New York, 1974).
- [44] J.C. Snijders and E.J. Baerends, *Mol. Phys.* 36 (1978) 1789.
- [45] J.G. Snijders, E.J. Baerends and P. Ros, *Mol. Phys.* 38 (1979) 1909.
- [46] J.H. Pollard, *Numerical and Statistical Techniques* (Cambridge Univ. Press, Cambridge, 1977).
- [47] G. Dahlquist, A. Björck and N. Anderson, *Numerical Methods* (Prentice-Hall, Englewood Cliffs, 1974).
- [48] B.R. Johnson, *J. Chem. Phys.* 67 (1977) 4086.
- [49] J.M. Blatt, *J. Comput. Phys.* 1 (1967) 382.
- [50] J.L. Dehmer, J. Berkowitz, L.C. Cusachs and H.S. Aldrich, *J. Chem. Phys.* 61 (1974) 594.
- [51] M.F. Lappert, J.B. Pedley, G.J. Sharp and N.P.C. Westwood, *J. Electron Spectry*, 3 (1974) 237.
- [52] E.J. Baerends, J.G. Snijders, C.A. de Lange and G. Jonkers, *Local Density Approximations in Quantum Chemistry and Solid State Physics*, eds. J.P. Dahl and J. Avery (Plenum Press, New York, 1984).
- [53] W. von Niessen, *J. Electron Spectry*, 37 (1985) 187.
- [54] D.M. de Leeuw, R. Mooyman and C.A. de Lange, *Chem. Phys. Letters* 54 (1978) 231.
- [55] J.M. Dyke, G.D. Josland, R.A. Lewis and A. Morris, *Mol. Phys.* 44 (1981) 967.
- [56] K.P. Huber and G. Herzberg, *Molecular Spectra and Molecular Structure*, Vol. 4. Constants of Diatomic Molecules (Van Nostrand, New York, 1979).
- [57] H.E. White, *Introduction to Atomic Spectra* (McGraw-Hill, New York, 1985).
- [58] C.E. Moore, *Atomic Energy Levels*, Vol. 1. Natl. Bur. Stand. Circ. 467 (US Govt. Printing Office, Washington, 1949).